



**HAL**  
open science

## Design and control of pressure-swing distillation for separating ternary systems with three binary minimum azeotropes

Ao Yang, Weifeng Shen, Shun'An Wei, Lichun Dong, Jie Li, Vincent Gerbaud

► **To cite this version:**

Ao Yang, Weifeng Shen, Shun'An Wei, Lichun Dong, Jie Li, et al.. Design and control of pressure-swing distillation for separating ternary systems with three binary minimum azeotropes. *AIChE Journal*, 2019, 65 (4), pp.1281-1293. 10.1002/aic.16526 . hal-02161001

**HAL Id: hal-02161001**

**<https://hal.science/hal-02161001>**

Submitted on 20 Jun 2019

**HAL** is a multi-disciplinary open access archive for the deposit and dissemination of scientific research documents, whether they are published or not. The documents may come from teaching and research institutions in France or abroad, or from public or private research centers.

L'archive ouverte pluridisciplinaire **HAL**, est destinée au dépôt et à la diffusion de documents scientifiques de niveau recherche, publiés ou non, émanant des établissements d'enseignement et de recherche français ou étrangers, des laboratoires publics ou privés.



## Open Archive Toulouse Archive Ouverte (OATAO)

OATAO is an open access repository that collects the work of Toulouse researchers and makes it freely available over the web where possible

This is an author's version published in: <http://oatao.univ-toulouse.fr/24029>

**Official URL:** <https://doi.org/10.1002/aic.16526>

**To cite this version:**

Yang, Ao and Shen, Weifeng and Wei, Shun'an and Dong, Lichun and Li, Jie and Gerbaud, Vincent  *Design and control of pressure-swing distillation for separating ternary systems with three binary minimum azeotropes.* (2019) *AIChE Journal*, 65 (4). 1281-1293. ISSN 0001-1541

Any correspondence concerning this service should be sent to the repository administrator: [tech-oatao@listes-diff.inp-toulouse.fr](mailto:tech-oatao@listes-diff.inp-toulouse.fr)

# Design and Control of Pressure-Swing Distillation for Separating Ternary Systems with Three Binary Minimum Azeotropes

Ao Yang , Weifeng Shen\* , Shun'an Wei and Lichun Dong

School of Chemistry and Chemical Engineering, Chongqing University, Chongqing, 400044, China

Jie Li

Centre for Process Integration, School of Chemical Engineering and Analytical Science, The University of Manchester, Manchester, U.K.

Vincent Gerbaud

LGC (Laboratoire de Génie Chimique), 4 allée Emile Monso, F-31432, Université de Toulouse, INP, UPS, Toulouse Cedex, 04, France

LGC (Laboratoire de Génie Chimique), F-31432, CNRS, Toulouse Cedex, 04, France

DOI 10.1002/aic.16526

*The separation of ternary nonideal systems with multi-azeotrope is very important because they are often found in the waste of chemical and pharmaceutical industries, which is much more difficult due to the formation of multi-azeotrope and distillation boundary. We propose a systematic procedure for design and control of a triple-column pressure-swing distillation for separating ternary systems with three binary minimum azeotropes. This procedure involves thermodynamic insights, a two-step optimization method, and effective control strategy. The separation of tetrahydrofuran (THF)/ethanol/water is used to illustrate the capability of the proposed procedure. It is found that the pressure limits in columns can be determined through the analysis of residue curve maps, distillation boundary, and isovolatility curves. The optimal triple-column pressure-swing distillation is generated with the minimum total annual cost (TAC) of  $\$2.181 \times 10^6$  in sequence A. The operating conditions are well controlled approaching their desired specifications in an acceptable time when disturbances occur.*

*Keywords:* triple-column pressure-swing distillation, ternary system, residue curve maps, optimization, temperature difference control strategy

## Introduction

The ternary nonideal system with three binary minimum azeotropes such as tetrahydrofuran (THF)/ethanol/water and acetonitrile/methanol/benzene is often found in chemical and pharmaceutical industries, requiring separation to avoid environmental issues.<sup>1,2</sup> However, the separation of such system is much more difficult than that of the binary azeotropic system and often leads to high capital and operating cost due to the existence of multi-azeotrope and multidistillation boundaries.<sup>2</sup>

The conventional distillation could not be used for the separation of such ternary nonideal system in most cases. There are three most common and important nonconventional distillations including pressure-swing, azeotropic, and extractive distillations that have been well developed for the separation of ternary nonideal mixtures in continuous modes. These distillations involve either changing operating pressures

(i.e., pressure-swing distillation)<sup>3-16</sup> or at another location instead (i.e., extractive distillation)<sup>17-21</sup> or adding an entrainer together with the feed (i.e., azeotropic distillation).<sup>22-24</sup> Although extractive distillations and azeotropic distillations can change the relative volatility of azeotropic mixtures by introducing an entrainer, some important characteristics of the entrainer such as solubility, toxicity, and stability require to be carefully investigated. Furthermore, the introduction of an entrainer may make the separation process of the ternary nonideal system with three azeotropes highly complicated and expensive due to the regeneration of the entrainer.<sup>25</sup> On the other hand, the pressure-swing distillation is used for the separation of pressure-sensitive azeotropes only through two or more columns in sequence at different pressures without introducing any entrainer. Therefore, it does not require recovery section for the entrainer. The energy and capital cost required in the pressure-swing distillation largely depends on the operating pressure, which could be significantly reduced through optimal design.

To optimally design an efficient pressure-swing distillation for the separation of ternary nonideal azeotropic mixtures, thermodynamic insights including design feasibility, sensitivity of design options over the whole composition, and

Additional Supporting Information may be found in the online version of this article.

Correspondence concerning this article should be addressed to W. Shen at shenweifeng@cqu.edu.cn

separation constraints are first generated through the analysis of well-drawn residue curve maps (RCMs).<sup>18-28</sup> There may exist several distillation boundaries on RCMs, dividing composition spaces into several distillation regions. A distillation region is defined as a feasible operating region when pure components or pressure-sensitive binary azeotrope(s) could be obtained at varying pressures.<sup>29</sup> Limiting values involving tangent pinches (e.g., pressures in different columns) and multi-distillation boundaries are quite important, which greatly affect flexibility, operability, and controllability of the pressure-swing distillation to achieve desired products. The search for limiting values is often carried out through an algebraic criterion or mathematical approaches like bifurcation theory.<sup>30</sup> Levy et al.<sup>31,32</sup> proposed an algebraic trial-and-error tangent pinch procedure for an extractive distillation to determine the minimum reflux ratio. Knapp and Doherty<sup>33</sup> applied bifurcation theory for the 1.0-1a class and related feasibility of an extractive distillation to the existence of saddle-node bifurcation points and branching points. Frits et al.<sup>34</sup> found an extractive distillation feasible under infinite reflux above a minimal entrainer flowrate corresponding to the merge of a stable pinch point originating from the azeotrope with a saddle point originating from a pure component. Recently, a unique noniterative method was proposed to locate possible split at finite reflux of azeotropic distillation based on the identification of common terminal points of pinch branches in each column section.<sup>35,36</sup> Although these methods are invaluable to find accurate limiting values, they are restricted to the separation of azeotropic mixtures with minimum (or maximum) boiling points belonging to the 1.0-1a class using extractive or azeotropic distillation with a heavy (or light) entrainer.

Feasibility studies were carried out for the separation of ternary systems using pressure-swing distillation. Modla and Lang<sup>13</sup> investigated feasibility of separating minimum and maximum azeotropes using pressure-swing batch distillation. The best batch distillation configuration was found through rigorous simulation. Modla and Lang<sup>37</sup> conducted dynamic simulation on the separation of acetone-methanol mixture using two pressure-swing batch distillation columns. The feasibility for the separation of ternary homoazeotropic mixtures using single and double pressure-swing batch distillation columns was investigated.<sup>38</sup> All these efforts are limited to pressure-swing batch distillation without providing detailed analysis of operating pressures, which may not be widely applicable to continuous pressure-swing distillation. Zhu et al.<sup>14</sup> reported a continuous triple-column pressure-swing distillation for separating acetonitrile/methanol/benzene nonideal azeotropic system and then they<sup>11</sup> studied heat integration and control of a triple-column pressure-swing distillation process. Luyben<sup>15</sup> also investigated the plant-wide dynamic controllability of this complex, nonideal interacting process. Valuable insights on design feasibility, sensitivity analysis on design options (e.g., pinch points of pressures in different columns) with a visual representation over the whole composition, and valid separation constraints for continuous pressure-swing distillation have not yet been reported.

In this work, we propose a systematic procedure for optimal design and effective control of a triple-column pressure-swing distillation for the separation of ternary nonideal system with three binary minimum azeotropes. This systematic procedure mainly consists of thermodynamic insights, process optimization, and effective control strategy. Some feasibility rules (i.e., isovolatility lines and volatility order) that are valid for the extractive distillation are investigated for their application

to the pressure-swing distillation for the first time, which are used to identify feasible composition regions, possible separation sequences in each feasible region and feasible ranges for a given pressure. The following questions are tackled as crucial issues in the conceptual design: Is the separation of targeted mixtures feasible using the pressure-swing distillation? Which separation sequences are most suitable? What are the limits on operating pressures to achieve the minimum total annual cost? These thermodynamic insights including design feasibility, pinch points of pressures in different columns and separation constraints are then incorporated into a process optimization model, and optimal design is generated through sensitivity analysis (SA) and sequential quadratic programming (SQP) method. Finally, a robust control strategy with feedforward and dual temperature difference structure is proposed to maintain product purities in each column when disturbances take place. The separation of THF/ethanol/water is used to illustrate the capability of the proposed procedure.

### Triple-Column Pressure-Swing Distillation

Figure S1 (Supporting Information) illustrates a triple-column pressure-swing distillation process for separating a ternary nonideal azeotropic system with three binary minimum azeotropes. Three products are obtained at the bottom streams B1, B2, and B3 of columns C1–C3 under the pressure of  $P_1$ ,  $P_2$ , and  $P_3$ , respectively.

### Systematic Design Procedure

The proposed systematic design procedure for optimal design and effective control of the proposed triple-column pressure-swing distillation for separating a ternary system with three binary minimum azeotropes is illustrated in the Supporting Information Figure S2. First, limiting values are identified based on thermodynamic insights from the analysis of RCMs, ternary diagram of classes 3.0-2, and general thermodynamic feasibility criteria. Second, process optimization is performed using the SA and SQP solvers to obtain the optimal design including optimal operating conditions. Then, a robust control strategy is proposed to ensure that the system is well controlled close to the desired specifications in an acceptable time under the condition of disturbances. Finally, the optimal design and well-controlled triple-column pressure-swing distillation are obtained.

### Thermodynamic insights from RCMs

RCMs are one of the most useful graphical techniques that are often used to assist conceptual design.<sup>18-28</sup> The analysis of well-drawn RCMs can provide valuable insights into design feasibility, reveal sensitivity of design options with a visual representation over the whole composition, and help to identify separation constraints. Based on thermodynamic insights into the design feasibility from RCMs, suitable pinch points are researched to achieve optimal operational pressures.

### Thermodynamic insights from general thermodynamic feasibility criteria

A general thermodynamic feasibility criterion for the separation of binary azeotropic mixture (A-B) using the extractive distillation with infinite reflux ratio was reported by Rodriguez-Donis et al.<sup>21</sup> Existence of a residue curve connecting entrainer E to A (or B) following a decreasing (respectively increasing) temperature direction inside the region

where A (or B) is the most (respectively least) volatile component of the mixture. According to this general feasibility criterion, residue curves in RCMs along with the distillation stable separatrix determine the volatility order in each possible region. In this study, thermodynamic feasibility insights from the extractive distillation (i.e., isovolatility lines, RCMs, and volatility orders) are extended for pressure-swing distillation to locate pinch points of pressures in different columns. Accordingly, the following significant questions are raised and required to be answered: Is the separation of targeted mixtures feasible using pressure-swing distillation? Which separation sequences are most suitable? What are the limits on operating pressures to achieve the minimum total annual cost?

### ***Thermodynamic insights into the separation of classes 3.0-2***

Thermodynamic insights into separating some Serafimov's classes including 1.0-1a, 1.0-1b, 1.0-2 (one azeotrope), 2.0-1, 2.0-2a, 2.0-2b, and 2.0-2c (two azeotropes) were well got through combining the knowledge of thermodynamic properties of RCMs and of the location of isovolatility and unidistribution curves.<sup>18-28,39-41</sup> The ternary system with a minimum boiling azeotrope and two intermediate boiling azeotropes belongs to Serafimov's class 3.0-2,<sup>42</sup> which can account for 8.4% of ternary azeotropic mixtures.<sup>43</sup> Different Serafimov's classes are illustrated in the Supporting Information Figure S3 with the Serafimov's class 3.0-2 in the Supporting Information Figure S3m.

Supporting Information Figure S4a shows some essential topological features for the class 3.0-2, corresponding to the separation of a ternary mixture A-B-C with three binary minimum azeotropes. While the A-B azeotrope with minimum boiling point denoted as  $UN_{RCM}$  is a RCM unstable node (hollow circle), the B-C and A-C azeotropes (denoted as  $S_{RCM1}$  and  $S_{RCM2}$ , respectively) are both RCM saddle points (hollow triangle) because there is no residue curve entering or going out. All three products A, B, and C are RCM stable nodes (black dot). All residue curves in a distillation region are directed from RCM unstable node to RCM stable node. From the Supporting Information Figure S4a, it can also be observed that two RCM stable separatrices divide the triangle composition space into three different distillation regions (i.e., Regions 1–3). Four possible volatile orders including  $ACB$ ,  $ABC$ ,  $BAC$ , and  $BCA$  can be identified through three isovolatility curves, which are represented by  $\alpha_{BC} = 1$ ,  $\alpha_{AB} = 1$ , and  $\alpha_{AC} = 1$ . Of note is that the triple-column pressure-swing column is feasible when the unstable or stable node toward to singular point of non-azeotrope or pure component exists for each component. These three isovolatility curves are highlighted in pink, each starting from an azeotropic point and ending at a point on a triangle side. The volatile order such as  $ACB$  indicates B is the first possible bottom product. From the Supporting Information Figure S4a, it can be clearly seen that the volatility order  $ACB$  is located at the upper section of the isovolatility curve  $\alpha_{BC} = 1$  within Region 1, indicating B is first possible bottom product in this section. Similar analysis can be carried out for the volatility orders  $ABC$ ,  $BAC$ , and  $BCA$ .

Figure S4b (Supporting Information) illustrates component balance lines for separating ternary nonideal mixtures into three constituent pure components through pressure-swing distillation. As shown in the Supporting Information Figure S4b, three products A, B, and C with high purities can be obtained at the bottom of three columns with different pressures. The fresh feed denoted as F with a feed composition of  $x_F$  is mixed

with the recycled stream denoted as D3 with a composition of  $x_{D3}$  from the overhead of the third column as an input (denoted as Mix) for the first column, which operates at pressure  $P_1$ . The feed stream Mix with a composition of  $x_{Mix}$  is separated into bottom product denoted as B1 with a purity of  $x_{B1}$  and overhead nonproduct stream denoted as D1 with a purity of  $x_{D1}$ . Stream D1 is fed into the second column at the pressure  $P_2$  to obtain product C with high purity of  $x_{B2}$  at the bottom and a near azeotropic mixture D2 with a purity of  $x_{D2}$  on the top. The azeotropic mixture D2 is fed into the third column operating at pressure  $P_3$ , high purity of product A,  $x_{B3}$ , is obtained at the bottom and a top distillate D3 with a purity of  $x_{D3}$ , which is close to the RCM stable separatrix at  $P_3$  is then recycled to the first column.

As demonstrated in the Supporting Information Figure S4a, isovolatility curves are used to define possible volatile orders in their respective regions, whereas RCM stable separatrices determine whether possible products could be actually obtained in their respective regions (Supporting Information Figure S4b). Following the suggestion of Knapp and Doherty,<sup>44</sup> the preferred feed composition in pressure-swing distillation is the minimum recycle-to-fresh feed ratio through locating the recycle stream composition in the RCM region where the distillation boundaries shift most with changing pressure and simultaneously maximize product flowrates by positioning the nonproduct streams (i.e., D1, D2, and D3) close to their respective boundaries. In this work, the effects of pressures on recycle-to-fresh ratio and product flowrates are investigated through SA to generate minimum values of recycle-to-fresh feed ratio and maximum product flowrates.

### ***Process optimization***

In this work, process optimization of the proposed triple-column pressure-swing distillation is carried out using the SA and SQP solvers.

**Objective Function.** Total annual cost (TAC) is often used as the objective function in the process design such as design of extractive distillation and pressure-swing distillation,<sup>11,12,16-20</sup> which is calculated using the following correlation from Douglas<sup>45</sup> (see Eq. 1).

$$TAC = \frac{\text{total capital cost}}{\text{payback period}} + \text{total operating cost} \quad (1)$$

The detailed capital cost formulas are shown in the Supporting Information Eqs. S1–S7. The payback period is assumed to be 3 years.<sup>46</sup> In additional, the utility cost is given in the Supporting Information Table S1.

**Constraints.** There are also numerous significant constraints including mass balance, energy balance, and thermodynamics, which are implicitly implemented in Aspen Plus<sup>®</sup> simulator. These rigorous correlations are generally represented by the Supporting Information Eqs. S8–S9. In addition, the purities of three products at the bottoms denoted as  $x_{B1}$ ,  $x_{B2}$ , and  $x_{B3}$ , respectively, must meet their desired design specifications that are shown in the Supporting Information Eqs. S10–S12.

**Variable Bounds.** Lower and upper bounds of the feed locations ( $N_{F1}$ ,  $N_{F2}$ ,  $N_{F3}$ , and  $N_{Rec}$ ), reflux ratios ( $R_1$ ,  $R_2$ , and  $R_3$ ), and total number of stages ( $N_{T1}$ ,  $N_{T2}$ , and  $N_{T3}$ ) are given in the Supporting Information Eqs. S13–S22, which are determined using the SA.

In this work, the complete process optimization model is defined as **CPOM** consisting of objective function, constraints,

and variable bounds in Eq. 1 and in the Supporting Information Eqs. S8–S22. The optimal values for the three continuous variables and seven discrete variables are generated using the SQP and SA solvers.

*Two-Step Solution Approach.* The complete process optimization model, **CPOM**, can be directly solved using SQP solver to generate the optimal solution. We notice that it is quite difficult to converge for SQP in Aspen Plus<sup>®</sup> with unknown operating pressures. To speed up the convergence of SQP, a two-step solution approach is proposed, which is demonstrated as follows.

*Step 1:* We first generate the possible pressures of each column in the feasible pressure range starting from the lowest allowable pressure that could be expressed as  $n \times 0.05$  MPa ( $n$  is an integer) with a step size of 0.05 MPa until the maximum allowable pressure is reached. In other words, we first examine those pressures that can be expressed as  $n \times 0.05$  MPa ( $n$  is an integer) in the feasible range. Note that the minimum and maximum allowable pressures are also included if they cannot be expressed as  $n \times 0.05$  MPa ( $n$  is an integer). Then, all possible pressure combinations of the three columns can be generated. Each combination is called as a scenario. For instance, if pressures  $P_2$  and  $P_3$  in each column are within [0.10, 0.20] MPa, three possible pressures of each column within the pressure range could be obtained starting from 0.10 MPa that could be expressed as  $2 \times 0.05$  MPa, resulting in total 9 ( $3 \times 3$ ) pressure combinations (or scenarios). Process optimization is conducted for each scenario with known operating pressures using SQP method and optimal solution is obtained.

*Step 2:* Comparing the optimal solution from each scenario, we can identify the pressure ranges where further possible reduction in the objective function could be achieved. Note that these pressure ranges are reduced much more compared to those in Step 1. Within those reduced pressure ranges, we generate all possible pressure combinations with a step size of 0.01 MPa and conduct optimization using SQP method again to obtain better solutions. In other words, we generate all possible pressure combinations within the neighborhood of the best solution obtained in Step 1 with a step size of 0.01 MPa.

### Control strategy

The key issue in the control of triple-column pressure-swing distillation process is how to maintain expected product purities when disturbances occur. Conventional single-loop temperature control strategy could not well control the process to achieve our desired conditions.<sup>15</sup> Thus, feedforward and dual temperature difference structure is proposed to effectively reduce deviations and offsets of products purities based on the singular value decomposition (SVD). In this study, we assume that the column has  $n$  stages. Hence, the steady-state gain matrix,  $\mathbf{K}$ , has  $n$  rows and  $m$  columns ( $m$  represents the number of manipulated variables), and it can be calculated through Eq. 2. Finally, the obtained gain matrix  $\mathbf{K}$  can be decomposed via the SVD in MATLAB (see Eq. 3).<sup>47</sup>

$$\mathbf{K} = \Delta \mathbf{C}_V / \Delta \mathbf{M}_V \quad (2)$$

$$\mathbf{K} = \mathbf{U} \Sigma \mathbf{V}^T \quad (3)$$

where  $\Delta \mathbf{C}_V$  is the change in stage temperatures and  $\Delta \mathbf{M}_V$  is the step change in manipulated variables,  $\mathbf{K}$  is the steady-state gain matrix,  $\mathbf{U}$  and  $\mathbf{V}$  are the orthonormal matrices, and  $\Sigma$  is a diagonal matrix of singular values.

## Computational Studies

The separation of THF/ethanol/water with three binary minimum azeotropes is used to illustrate the proposed design procedure. NRTL model is selected because its reliable binary interaction parameters (see in the Supporting Information Table S2) are well provided in the open literature.<sup>2</sup> Three binary minimum azeotropes of this system calculated from the NRTL model are consistent with those reported values, as shown in the Supporting Information Table S3. For the purpose of simplification, the feed flowrate is assumed to be 100 kmol/h with the compositions of THF, ethanol, and water corresponding to 33, 33, and 34 mol %, respectively.<sup>1</sup> The design procedure is also extended to other feed flowrates and compositions.

### Separation sequences

The moving trend of RCM stable separatrix with varying pressures from 0.10 to 1.00 MPa is shown in the Supporting Information Figure S5. From the Supporting Information Figure S5a, the trend of changes in the RCM stable separatrix of  $UN_{RCM}T_{min}azeo_{AB}-S_{RCM1}azeo_{BC}$  and  $UN_{RCM}T_{min}azeo_{AB}-S_{RCM2}T_{inter}azeo_{AC}$  is not obvious. The trend of changes in the RCM stable separatrix of  $UN_{RCM}T_{min}azeo_{AB}-S_{RCM2}T_{inter}azeo_{AC}$  has become increasingly apparent from 0.60 to 1.00 MPa (see Supporting Information Figure S5b). The RCM stable separatrix of  $UN_{RCM}T_{min}azeo_{AB}-S_{RCM2}T_{inter}azeo_{AC}$  and the azeotrope point of A-C disappear while the operating pressure is increased up to 1.00 MPa. The point of feed composition (red star) is always located in the region of  $S_{RCM1}azeo_{BC}-UN_{RCM}T_{min}azeo_{AB}-B$  while vary pressures from 0.10 to 1.00 MPa. It can be concluded that the pressure-swing distillation could be applied to separate ternary mixture water/THF/ethanol and water can be obtained as the possible product in the first column, whereas ethanol and THF can be obtained in the second and third columns.

To clearer display the separation sequences, the component balance lines are given in Figure 1. There are two possible separation sequences (labeled as A and B) for the separation of THF/ethanol/water system, which are call separation sequences A and B. As shown in Figure 1, three products water, ethanol, and THF with high purities (i.e.,  $x_{B1}$ ,  $x_{B2}$ , and  $x_{B3}$ ) can be obtained at the bottom of three columns with different pressures (i.e.,  $P_1$ ,  $P_2$ , and  $P_3$ ). The fresh feed composition of  $x_F$  is mixed with the recycled stream composition of  $x_{D3}$  as an input ( $x_{Mix}$ ) for the first column, which operates at pressure  $P_1$ . The point of  $x_{Mix}$  is separated into  $x_{B1}$  and  $x_{D1}$ . The point of  $x_{D1}$  is fed into the second column at the pressure  $P_2$  to obtain product ethanol with high purity of  $x_{B2}$  at the bottom of second column and a ternary azeotropic mixture D2 with a purity of  $x_{D2}$  on the top in the sequence A (Figure 1a). On the contrary, the product of THF can be obtained at the bottom of the second column in the sequence B (Figure 1b). Finally, the product of THF in sequence A and ethanol in sequence B can be obtained via the composition balance lines of third column. In this work, the preferred nonproduct stream compositions of D1, D2, and D3 (i.e.,  $x_{D1}$ ,  $x_{D2}$ , and  $x_{D3}$ ) are estimated via the ternary diagram and lever rule in the Supporting Information Figure S6.

*Sequence A: Water, Ethanol, and THF.* The triple-column pressure-swing distillation process with sequence A is illustrated in the Supporting Information Figure S7. Water is first obtained at the bottom of column C1 under the pressure of  $P_1$ . Then ethanol product could be generated at the bottom of column C2 at  $P_2$ . Finally, THF is produced at the bottom of the third column C3 at  $P_3$ .

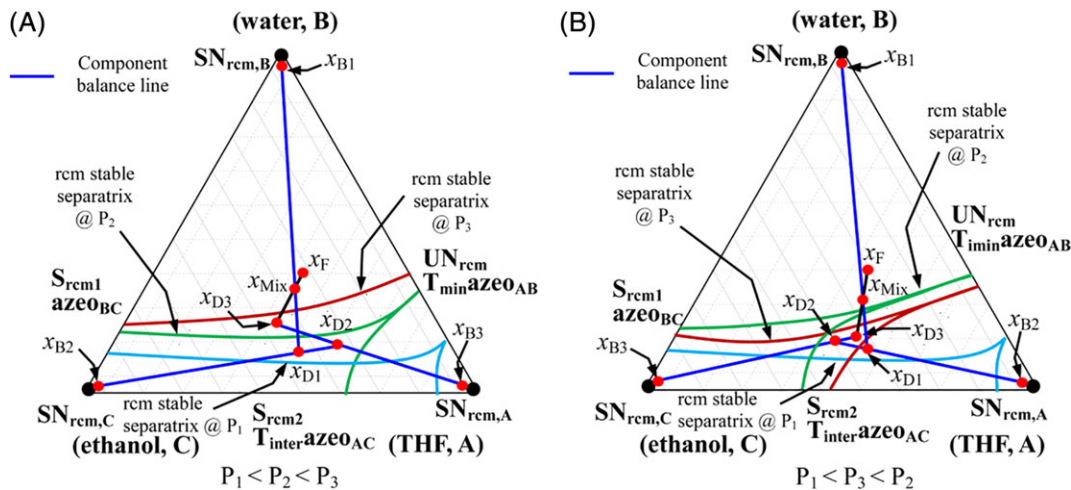


**Figure 1.** The component balance lines of (a) sequence A and (b) sequence B for separating water/THF/ethanol non-ideal azeotropic system.

[Color figure can be viewed at wileyonlinelibrary.com]

The topological features for the separation of water/ethanol/THF mixture in column C1 are illustrated in Figure 2. As shown in Figure 2a, the isovolatility curve  $\alpha_{BC} = 1$  separates the region as volatility orders  $ACB$  and  $ABC$  because THF interacts differently with water and ethanol. The upper section refers to the enclosed area  $ACB$  surrounded by purple dotted lines, whereas the lower section refers to the enclosed area  $ACB$  surrounded by black dotted lines in Region 1. The desired water product (B) can be achieved at the bottom of C1 only if the feed point denoted as Mix with  $x_{Mix}$  is located at the upper section of the triangular composition in Region 1. Otherwise, the water product could not be obtained from the first bottom stream while the  $x_{Mix}$  is located within the lower section in Region 1. The moving trends of RCM stable separatrix and the curve  $\alpha_{BC} = 1$  along with pressures varying from 0.10 to 0.30 MPa is clearly demonstrated in Figure 2a. When the operating pressure of column C1 changes from 0.10 to 0.20 MPa, the feed point Mix is located in the upper section of the isovolatility curve  $\alpha_{BC} = 1$  at 0.20 MPa. However, it is located in the lower part of the triangular composition diagram

after passing across the isovolatility curve  $\alpha_{BC} = 1$  at 0.30 MPa when the operating pressure of column C1 increases to 0.30 MPa. If the operating pressure of 0.20 MPa is selected, Region 1 will become smaller, and the separation therefore will become more difficult. The optimal pressure 0.10 MPa is well qualified for separating water from water/ethanol/THF mixture in column C1.

The fresh feed point F with  $x_F$ , the bottom product composition  $x_{B1}$ , recycle stream feed point D3 with  $x_{D3}$ , and total feed point Mix are illustrated in Figure 2b. The fresh feed point F with  $x_F$  representing the total feed that is fed into column C1, the bottom product B1 represents water with high-purity at the upper corner A of the triangular composition diagram, total feed Mix refers to the mixing of the fresh feed and the recycle feed stream. The composition at Mix is calculated using Eq. 4. Based on the component balance line in Region 1, the point D1 is located on the extension of the line joining B1 and Mix according to Eq. 5 indicating a high-purity water could be easily obtained at Eq. 5 indicating a high-purity water could be easily obtained at the bottom of column C1 with the pressure of 0.10 MPa. The cooling water at 298.15 K and low-pressure

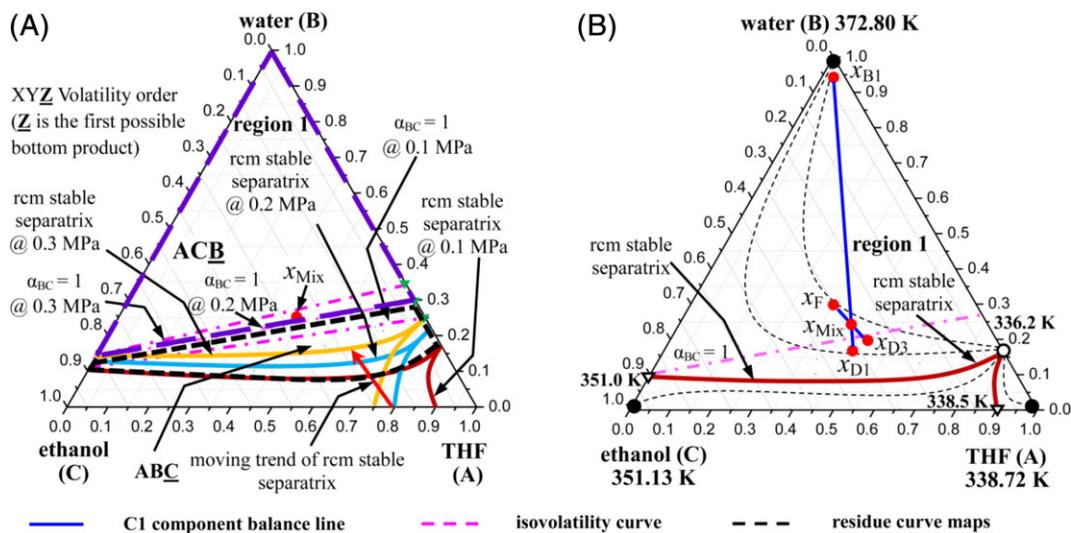


**Figure 2.** Topological features for the separation of water/ethanol/THF in column C1.

(a) Moving trend of RCM stable separatrix and  $\alpha_{BC} = 1$  when the pressure changes from 0.10 to 0.30 MPa and (b) at 0.10 MPa. [Color figure can be viewed at wileyonlinelibrary.com]

steam at 433.15 K can be used in the condenser and reboiler whose temperature are set as 340.4 and 375.65 K at the operating pressure of 0.10 MPa, respectively.

$$F_F \cdot x_F + F_{D3} \cdot x_{D3} = F_{\text{Mix}} \cdot x_{\text{Mix}} \quad (4)$$

$$F_{B1} \cdot x_{B1} + F_{D1} \cdot x_{D1} = F_{\text{Mix}} \cdot x_{\text{Mix}} \quad (5)$$

The topological features in column C2 are illustrated in Figure 3. The distillate D1 from column C1 is the main feed of column C2 at a higher pressure, crossing the RCM stable separatrix from Region 1 to Region 2. As shown in Figure 3a, the Region 2 is located between the isovolatility curves  $\alpha_{BC} = 1$  and  $\alpha_{AC} = 1$ . In this region, ethanol (C) is the first possible bottom product. To achieve a high-purity ethanol product, it is necessary to ensure the point D1 to be located in the region 2. The point D1 is getting close to the RCM stable separatrix at 0.45 MPa when the operating pressure of column C2 gradually increases to 0.45 MPa (Figure 3a). As demonstrated in Figure 3b, the point D1 is able to cross exactly the distillation boundary and reach Region 2 when the operating pressure of column C2 is chosen as 0.45 MPa. It can be obviously

observed from Figure 3c that the point D1 will escape Region 2 when the pressure is greater than 0.75 MPa. Based on the lever rule, the  $x_{D2}$  and  $x_{B2}$  can be obtained in Region 2 (Figure 3d). Overall, the operating pressure should range from 0.45 to 0.75 MPa. The optimal value will be determined through the following process optimization.

The topological features in column C3 are illustrated in Figure 4. The distillate D2 from column C2 is the main feed of column C3 at a different pressure, crossing the RCM stable separatrix from Region 2 at the previous pressure to the new Region 3 at 0.75 MPa. Following of our previous study,<sup>19,46</sup> the  $\alpha_{AC} = 1$  curve intersects the binary side AB while the intersection point is called  $x_{P, AC}$ . As represented in the Supporting Information - Table S4, the composition point of  $x_{P, AC}$  is located on the THF-ethanol side of the triangle with the THF composition of 0.146 at 0.80 MPa. However, its composition increases slightly to 0.150 at 0.90 MPa, stays at 0.150 under 0.95 MPa, and disappears at 1.00 MPa. Therefore, the isovolatility curve  $\alpha_{AC} = 1$  in Region 3 is not qualified to accurately describe the volatility order. To obtain a high-purity ethanol product, the point D2 is expected to be located in the Region 3.

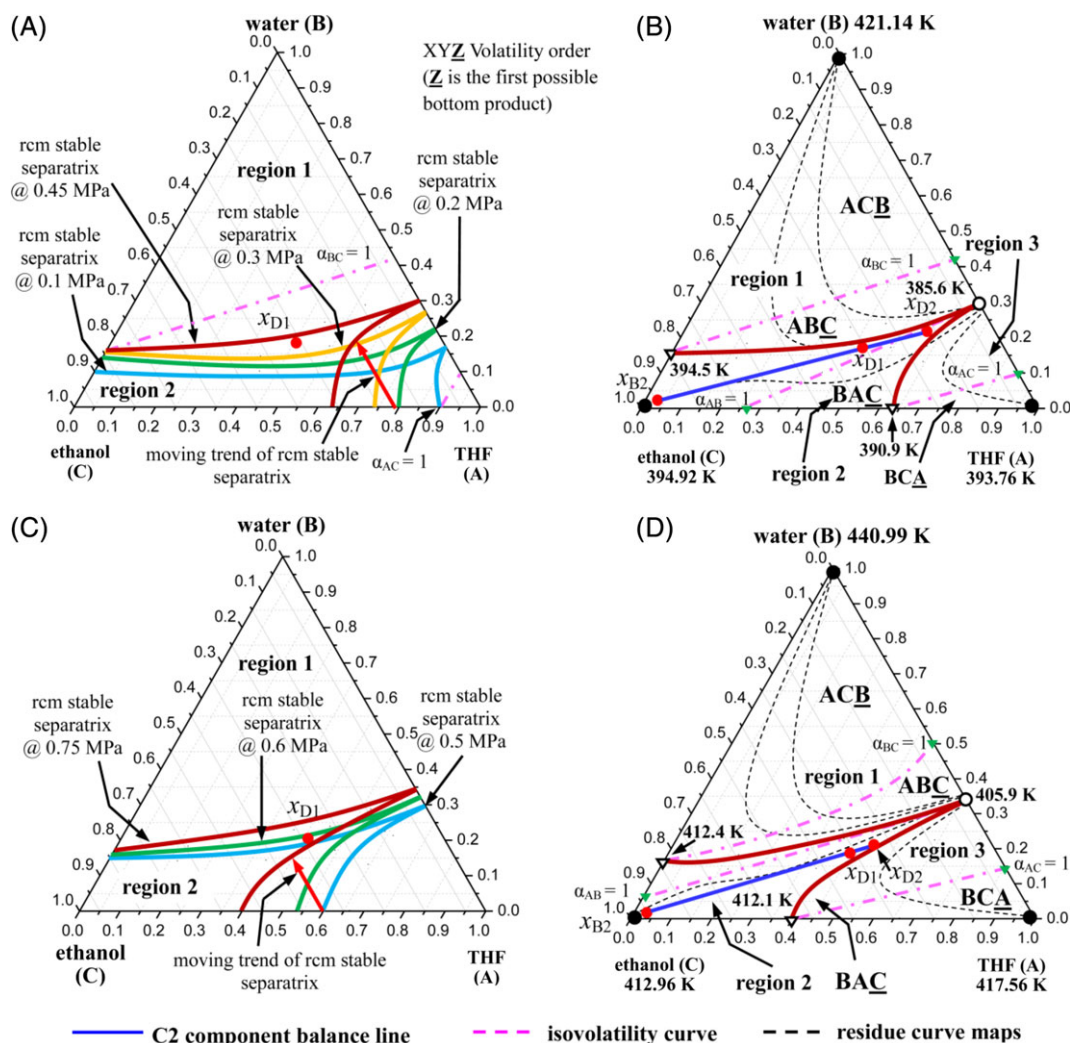


Figure 3. Topological features for the separation of water/ethanol/THF mixture in column C2.

(a) Moving trend of RCM stable separatrix with varying pressures from 0.10 to 0.45 MPa, (b) at 0.45 MPa, (c) moving trend of RCM stable separatrix with varying pressures from 0.50 to 0.75 MPa, and (d) at 0.75 MPa. [Color figure can be viewed at wileyonlinelibrary.com]

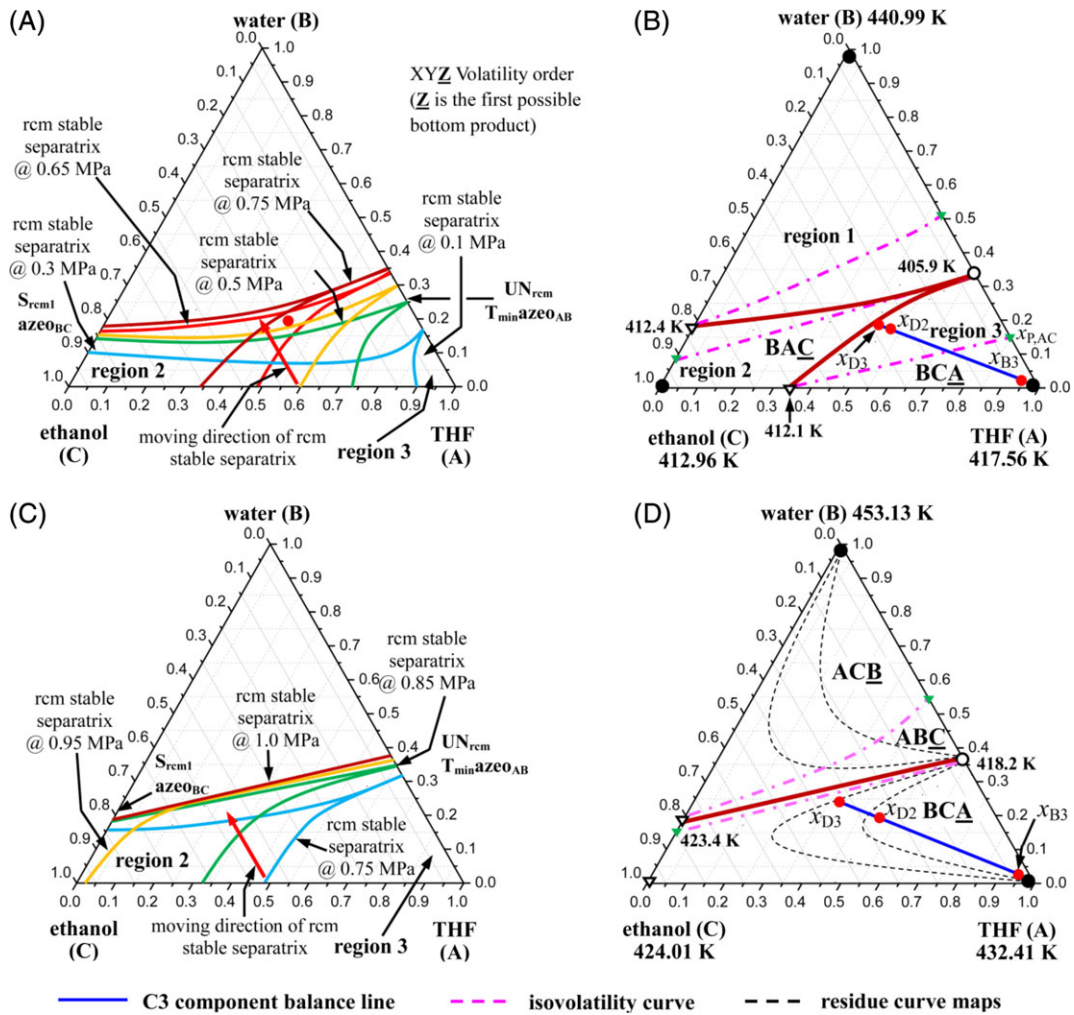


Figure 4. Topological features for the separation of water/ethanol/THF in column C3.

(a) Moving trend of RCM stable separatrix with varying pressures from 0.10 to 0.75 MPa, (b) at 0.75 MPa, (c) moving trend of RCM stable separatrix with varying pressures from 0.75 to 1.00 MPa, and (d) at 1.00 MPa. [Color figure can be viewed at [wileyonlinelibrary.com](http://wileyonlinelibrary.com)]

$$F_{B3} \cdot x_{B3} + F_{D3} \cdot x_{D3} = F_{D2} \cdot x_{D2} \quad (6)$$

As shown in Figure 4a, the nonproduct stream D2 approaches the RCM stable separatrix when the operating pressure of column C3 increases from 0.10 to 0.75 MPa. As demonstrated in Figure 4b, the point D2 reaches Region 3 when the operating pressure of column C3 is selected as 0.75 MPa. Based on the lever rule in Eq. 6, the point D3 is located on the extension of line segment B3-D2. From Figure 4c, the moving distance of distillation boundaries  $S_{RCM2} T_{inter,azeoBC} - UN_{RCM} T_{min,azeoAB}$  along the binary side ethanol-THF when the pressure increases from 0.75 to 0.95 MPa is significantly larger than that when the pressure increases from 0.95 to 1.00 MPa or even more. The pressure above 1.00 MPa has little effect on the separation. The  $x_{D3}$  and  $x_{B3}$  can be obtained based on the component balance line in column C3 (Figure 4d). Therefore, the operating pressure of column C3 ranges between 0.75 and 1.00 MPa. The optimal value is identified through the following optimization.

**Sequence B: Water, THF, and Ethanol.** The triple-column pressure-swing distillation process with separation sequence B is illustrated in the Supporting Information Figure S8. The nonproduct stream D3 from column C3 is recycled and mixed

with the fresh feed to form the feed to column C1, which is operated at pressure  $P_1$ . High-purity water product is obtained at the bottom of column C1. The distillate D1 of column C1 is fed to the column C2 (operating at pressure  $P_2$ ), where it is separated into pure THF and the distillate D2. The distillate D2 is fed into column C3 with the operating pressure of  $P_3$ , where ethanol product is obtained at the bottom.

Figure 5 illustrates the topological features for the separation of THF/ethanol/water with sequence B in the column C1. The expected operating pressure for column C1 is strictly identical to that with sequence A as both of them have the same bottom product. The detailed analysis is very similar to that with sequence A and hence could be referred to *Section Sequence A: Water, ethanol, and THF*. The optimal operating pressure of 0.10 MPa is identified for column C1 to ensure Mix point reaches Region 1 located in the upper section (enclosed area  $ACB$  surrounded by purple dotted lines) of the triangle and above the isovolatility curve  $\alpha_{BC} = 1$ .

The distillate D1 from column C1 with a lower pressure  $P_1$  is fed into column C2, which has a higher pressure  $P_2$ , crossing the RCM stable separatrix from Region 1 at  $P_1$  to Region 2 at  $P_2$ . The composition point of  $x_{P,AC}$  (i.e.,  $x_{P,AC} = 0.146$ ) is located on the triangle side THF-ethanol when the operating

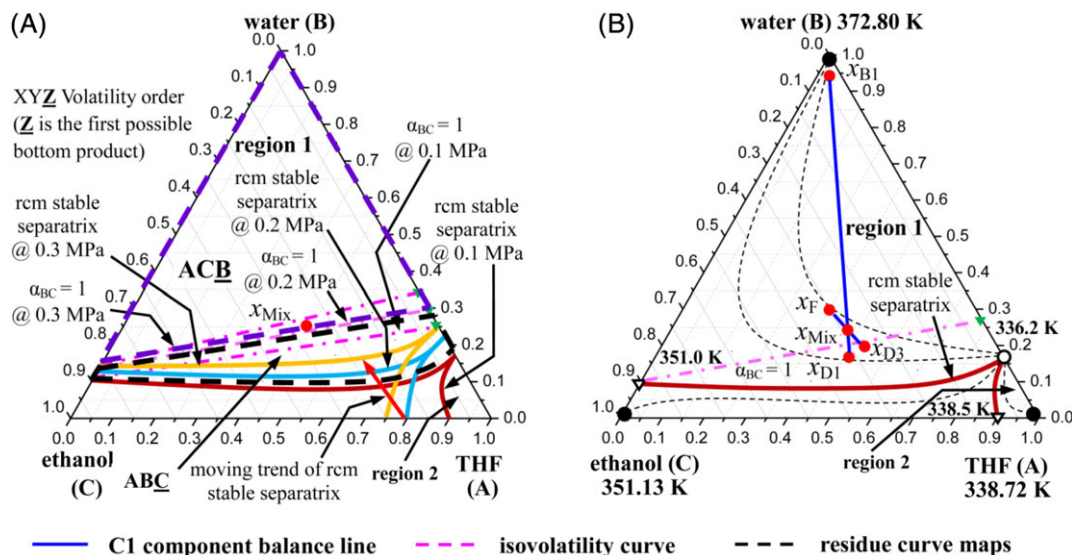


**Figure 5. Topological features for the separation of water/THF/ethanol with sequence B in column C1.**

(a) Moving trend of RCM stable separatrix and  $\alpha_{BC} = 1$  with varying pressures from 0.10 to 0.30 MPa and (b) at 0.10 MPa. [Color figure can be viewed at [wileyonlinelibrary.com](https://onlinelibrary.wiley.com)]

pressure is set as 0.80 MPa (Supporting Information Table S4). It gets very close to the point with a composition of 0.150 on the THF-ethanol side when the operating pressure increases from 0.80 to 0.95 MPa. However, it disappears from the THF-ethanol side when the pressure is increased to 1.00 MPa (Supporting Information Table S4). At this situation, the isovolatility curve  $\alpha_{AC} = 1$  is no longer used to accurately describe the volatility order in Region 2. However, RCM stable separatrix boundaries still could be used to judge which product could be actually obtained in the desired region, requiring D1 point to be located in Region 2 in order to generate a high-purity ethanol product.

The moving trend of RCM stable separatrix boundaries along with varying pressures from 0.10 to 0.80 MPa is shown in Figure 6a. As shown in Figure 6a, the point D1 with a composition of  $x_{D1}$  is located near the RCM stable separatrix at 0.80 MPa, indicating the separation of THF is possible. As demonstrated in Figure 6b, the composition of point D1 could be separated into  $x_{D2}$  and  $x_{B2}$  when the operating pressure of column C2 is selected as 0.80 MPa. The point D1 is able to pass across the distillation boundary and reach the desired Region 2 while the pressure of column C2 is greater than or equal to 0.80 MPa. From Figure 6c, the moving distance of the distillation boundaries  $S_{RCM1} \alpha_{BC} - UN_{RCM} T_{min} \alpha_{zeoAB}$  along the triangle side ethanol-water when the pressure increases from 0.80 to 0.95 MPa is significantly larger than that when the pressure is increased from 0.95 to 1.00 MPa or more (Supporting Information Table S4). The pressure has little effect on the separation process when it is above 1.00 MPa. The distillate stream (D2) of column C2 is located at Region 2 when the operating pressure is under 1.00 MPa as illustrated in Figure 6d. In a brief, the preliminary range for the operating pressure of column C2 is between 0.80 and 1.00 MPa. Its optimal value is identified through optimization.

It can be concluded from *Section Sequence A: Water, ethanol, THF* that the point D2 crosses the RCM stable separatrix of Region 2 and reaches Region 3 when the pressure increases from  $P_2$  to  $P_3$ . Note that Region 3 is located between the isovolatility curves  $\alpha_{BC} = 1$  and  $\alpha_{AC} = 1$ , where ethanol product (C) is the first possible bottom product. Therefore, it must

ensure the point D2 to be located in Region 3 to obtain a high-purity ethanol product.

Figure 7a gives the moving trend of the RCM stable separatrix when the pressure varies from 0.10 to 0.50 MPa. The point D2 with a composition of  $x_{D2}$  is located near the RCM stable separatrix at 0.50 MPa indicating the separation of product ethanol is possible. As shown in Figure 7b, the composition of point D2 is divided into  $x_{D3}$  and  $x_{B3}$  when the operating pressure of column C3 is determined at 0.50 MPa. Similar observations can be made for the upper bounds of  $P_3$  from parts c–d of Figure 7. As a result, the operational pressure of column C3 should be selected between 0.50 and 0.80 MPa. Its optimal value is determined through optimization.

### Optimization results

Based on the aforementioned analysis, the pressures of C1–C3 (i.e.,  $P_1$ ,  $P_2$ , and  $P_3$ ) are within [0.10, 0.10], [0.45, 0.75], and [0.75, 1.00] MPa, respectively, for sequence A, whereas they are within [0.10, 0.10], [0.80, 1.00], and [0.50, 0.80] MPa, respectively, for sequence B. It can be concluded that there are totally 42 pressure combinations for sequence A and totally 35 pressure combinations for sequence B. All scenarios are solved on the desktop with Intel Core i7-6700HQ CPU @ 2.60GHZ RAM 8 GB using Windows 10. The computational time is set about 6 h for each scenario.

However, some scenarios are infeasible which are validated in Aspen Plus because the corresponding feed compositions are close to distillation boundaries in the ternary diagram. All feasible and infeasible scenarios for sequences A and B are indicated in the Supporting Information Tables S5 and S6, respectively. It can be seen that there are 11 feasible scenarios for sequence A and 7 for sequence B. Each feasible scenario is labeled where the first capital A stand for sequence A and the first capital B stands for sequence B as indicated in the Supporting Information Tables S5 and S6.

The lower and upper bounds of operating variables in the CPOM for A1<sup>#</sup>–A11<sup>#</sup> is given in the Supporting Information Tables S7–S17. The optimal results for scenarios A1<sup>#</sup>–A11<sup>#</sup> are presented in the Supporting Information Table S18. The minimum TAC of  $\$2.615 \times 10^6$  is obtained in A4<sup>#</sup> where

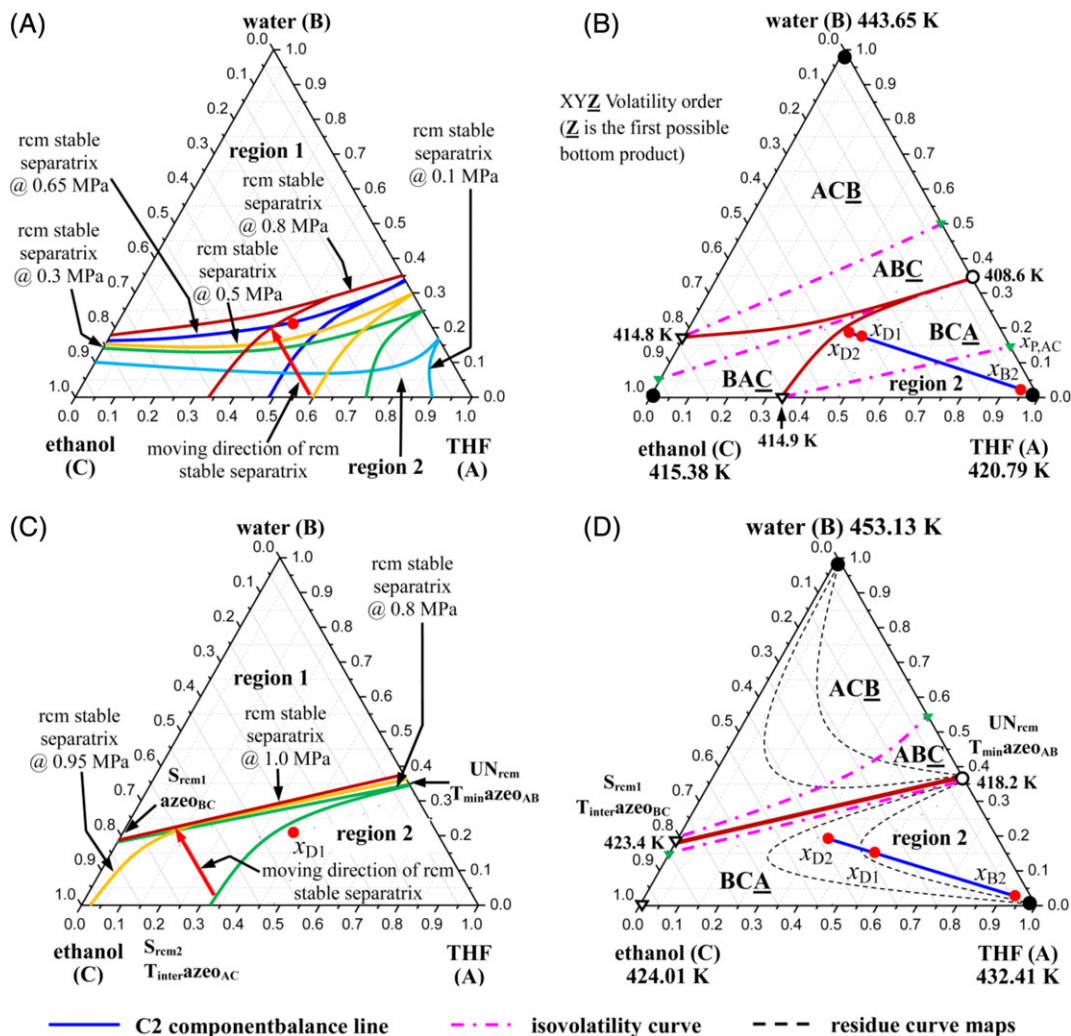


**Figure 6. Topological features for the separation of water/THF/ethanol with sequence B in column C2.**

(a) Moving trend of RCM stable separatrix with varying pressures from 0.10 to 0.80 MPa, (b) at 0.80 MPa, (c) moving trend of RCM stable separatrix with varying pressures from 0.80 to 1.00 MPa, and (b) at 1.00 MPa. [Color figure can be viewed at [wileyonlinelibrary.com](http://wileyonlinelibrary.com)]

$P_1 = 0.10$  MPa,  $P_2 = 0.55$  MPa, and  $P_3 = 1.00$  MPa. From Supporting Information Table S18, it can be concluded that the TAC always increase when  $P_3$  decreases from 1.00 MPa to other pressures. However,  $P_3$  cannot increase because it reaches the maximum allowed pressure. When  $P_2$  increases from 0.55 MPa to other pressures, the TAC also increases. Therefore,  $P_2$  should decrease. Note that when  $P_2$  is reduced to 0.50 MPa, the pressure is infeasible as indicated in the Supporting Information Table S18. In a brief, the pressure ranges for  $P_1$ ,  $P_2$ , and  $P_3$  are reduced to [0.10, 0.10], (0.50, 0.55], and [1.00, 1.00]. Therefore, only five combinations (scenarios) can be obtained with a step size of 0.01 MPa, as listed in the Supporting Information Table S19.

The optimal solutions for these five scenarios are presented in the Supporting Information Table S19. From Supporting Information Table S19, it can be observed that the minimum TAC is about  $\$2.181 \times 10^6$  in A4<sup>#2\*</sup> where  $P_1 = 0.10$  MPa,  $P_2 = 0.52$  MPa, and  $P_3 = 1.00$  MPa. The optimal numbers of stage in C1–C3 are 29, 72, and 70, respectively. The corresponding design parameters of the optimal triple-column pressure-swing distillation with sequence A is illustrated in

Figure 8. Similar results and observations could be made for sequence B (Supporting Information Tables S6 and S20). Combined the results for sequences A and B, we can conclude that the scenario A4<sup>#2\*</sup> is the best with the minimum of TAC.

The liquid composition profiles in C1–C3 are illustrated in the Supporting Information Figures S9a–c, respectively. It can be observed from Supporting Information Figure S9a, there is a steep slope on the ethanol and water composition profiles in C1, indicating that much less number of stages is required for column C1 than those for C2 and C3 to achieve the desired purity. Meanwhile, Supporting Information Figure S9d demonstrates the ternary composition profiles of triple-column pressure-swing distillation process with composition points and feed locations of the streams and it could also be observed that the separation of THF and ethanol are more difficult because many trays are required in the stripping section profile of column C2 (marked as tangerine triangle points) and in the rectifying section profile of column C3 (marked as red square points).

Supporting Information Figure S10 illustrates temperature profiles in C1–C3, steady-state gain and SVD of column C2.

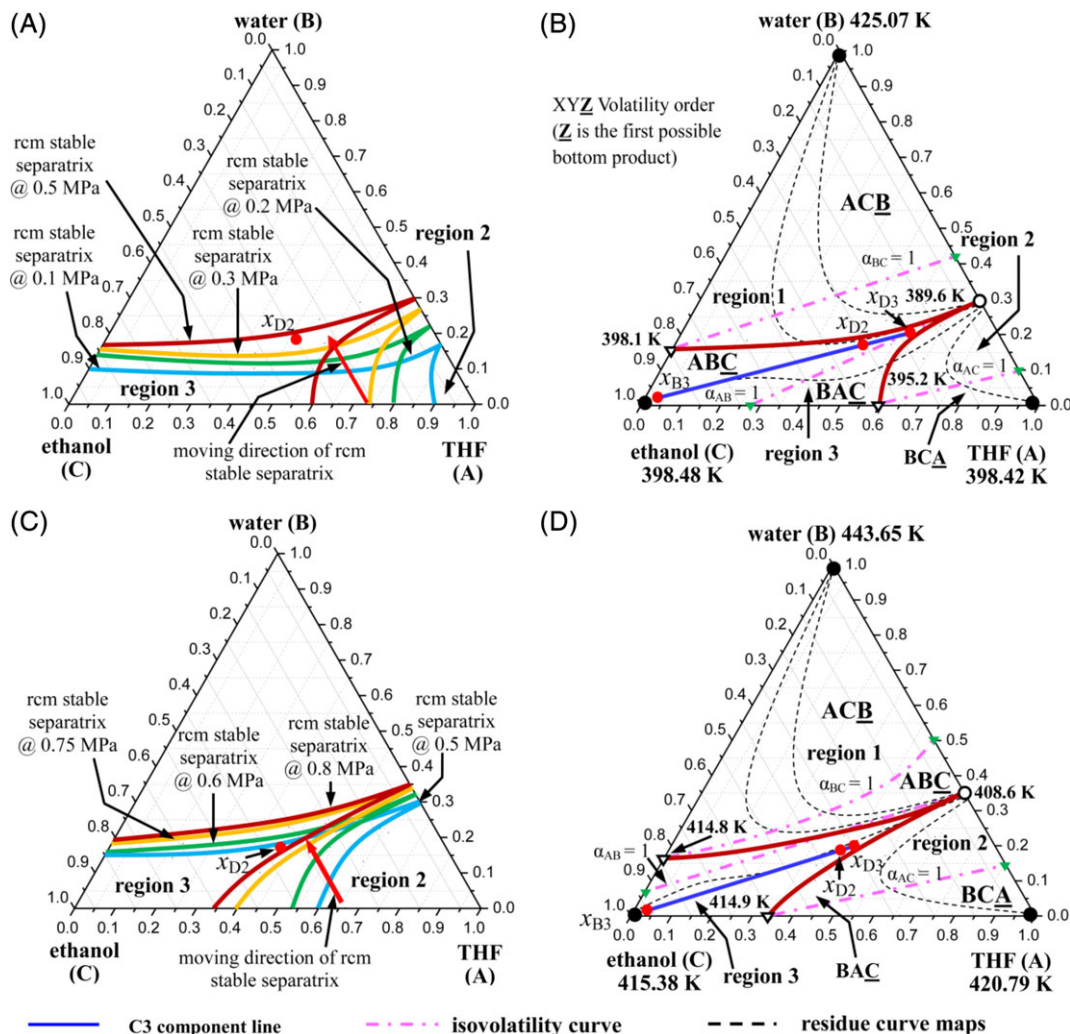


**Figure 7. Topological features for the separation of water/THF/ethanol with sequence B in column C2.**

(a) moving trend of RCM stable separatrix with varying pressures from 0.10 to 0.50 MPa, (b) at 0.50 MPa, (c) moving trend of RCM stable separatrix with varying pressures from 0.50 to 0.80 MPa, and (d) at 0.80 MPa. [Color figure can be viewed at [wileyonlinelibrary.com](http://wileyonlinelibrary.com)]

As shown in the Supporting Information Figure S10a,c, stage 27 in C1, and stage 61 in C3 are selected for the temperature control because significant temperature break takes place in these two stages.<sup>48,49</sup> However, the temperature profile in C2 is relatively flat, as illustrated in the Supporting Information - Figure S10b. It is not clear that which stage should be chosen for temperature control in C2. To determine the sensitive stage (SS) of the C2, the steady-state gains in the Supporting Information Figure S10d are obtained by varying +0.1% reboiler heat duty and reflux ratio of column C2. Next, the singular value  $U$  in the Supporting Information Figure S10e can be decomposed via the built-in SVD function in MATLAB. From the Supporting Information Figure S10e, temperatures on stages 25 and 39 are determined as SS. To choose the reference stage (RS), the singular value  $U$  in the Supporting Information Figure S10f can be obtained by decomposing the  $dT/dQ_{R2}-dT_{39}/dQ_{R2}$  and  $dT/dRR_2-dT_{25}/dRR_2$ . Following the suggestion of Ling and Luyben,<sup>47</sup> the insensitive stages and those are most close to SS could be determined as RS. As such, the stages 6 and 58 are determined as RS from the Supporting Information Figure S10f, while the  $\Delta T_{25} = (T_{25}-T_6)$

and  $\Delta T_{58} = (T_{58}-T_{39})$  can be constructed for the proposed robust dual temperature difference approach.

A plant-wide control structure with feedforward and dual temperature difference strategy is proposed in Figure 9 based on the basic control strategy in the Supporting Information Figure S11 for the triple-column pressure-swing distillation to effectively reduce deviations and offsets of products purities.<sup>11,15</sup> The detailed information (e.g., column diameter and side weir length) of three columns are given in the Supporting Information - Table S21. In this proposed structure, temperatures of tray 27 and 61 (i.e.,  $T_{27}$  and  $T_{61}$ ) are controlled by manipulating the ratios of  $Q_{R1}/F$  and  $Q_{R3}/D_2$  in columns C1 and C3, respectively. In addition, two temperature differences  $\Delta T_{25} = (T_{25}-T_6)$  and  $\Delta T_{58} = (T_{58}-T_{39})$  are controlled via two temperature controllers TDC1 and TDC2 to adjust the ratio of  $Q_{R2}/F$  and  $R_2/F$  in column C2 to effectively reduce the offsets of products purities. Furthermore, the gain and integral time of all temperature controllers are tuned by running a relay-feedback test with Tyreus-Luyben tuning rules and illustrated in the Supporting Information Table S22.

In this work, disturbances in feed flowrates (i.e.,  $\pm 10\%$  flowrate) and compositions (i.e., 34 and 32 mol % THF) are

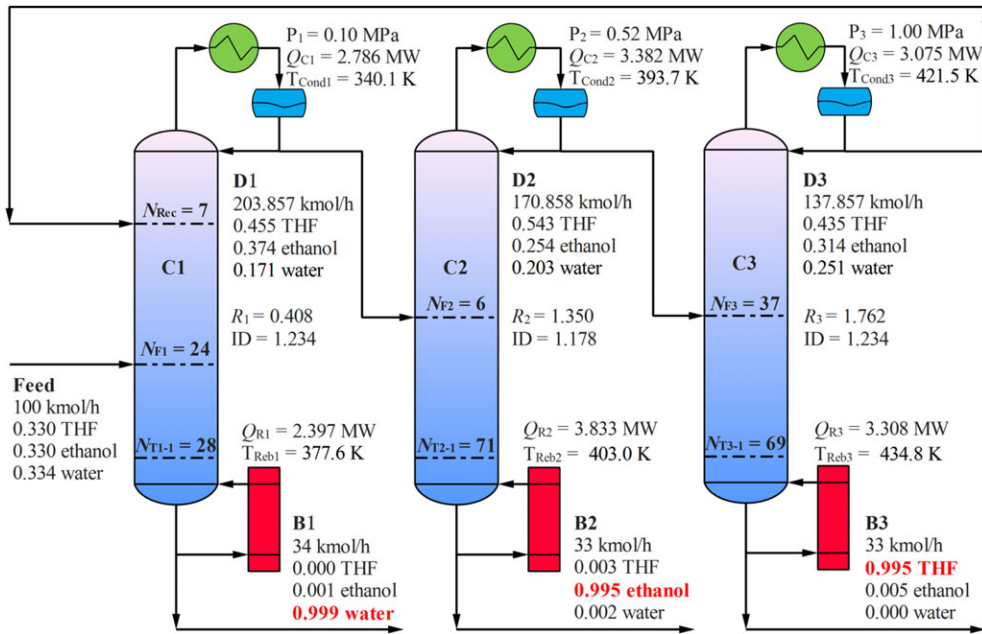


**Figure 8. Optimal triple-column pressure-swing distillation process with sequence A (A4<sup>#2</sup>).**  
 [Color figure can be viewed at [wileyonlinelibrary.com](http://wileyonlinelibrary.com)]

considered to evaluate the performance of the proposed plant-wide control structure. The dynamics of the product purities and the control temperature using the proposed control structure are illustrated in the Supporting Information Figures S14–S15.

As shown in the Supporting Information Figure S14, the dynamics of the bottom product purities in each column are represented by the red solid lines and blue dashed lines when the fresh feed flowrates increase by 10% and decrease by 10%, respectively. It can be observed that the purities of water, ethanol and THF are close to their desired values of

99.9, 99.5, and 99.5 mol % even through there is a fluctuation in the fresh feed flowrate by 10%.

The dynamics of product purities and controlled temperature using the proposed control structure for disturbances in compositions is illustrated in the Supporting Information Figure S15. The responses of the proposed plant-wide control structure to composition disturbances start at 1 h. Under the feed compositions disturbances in fresh feed, the purities of water, ethanol, and THF are controlled close to their desired values of 99.9, 99.5, and 99.5 mol %.

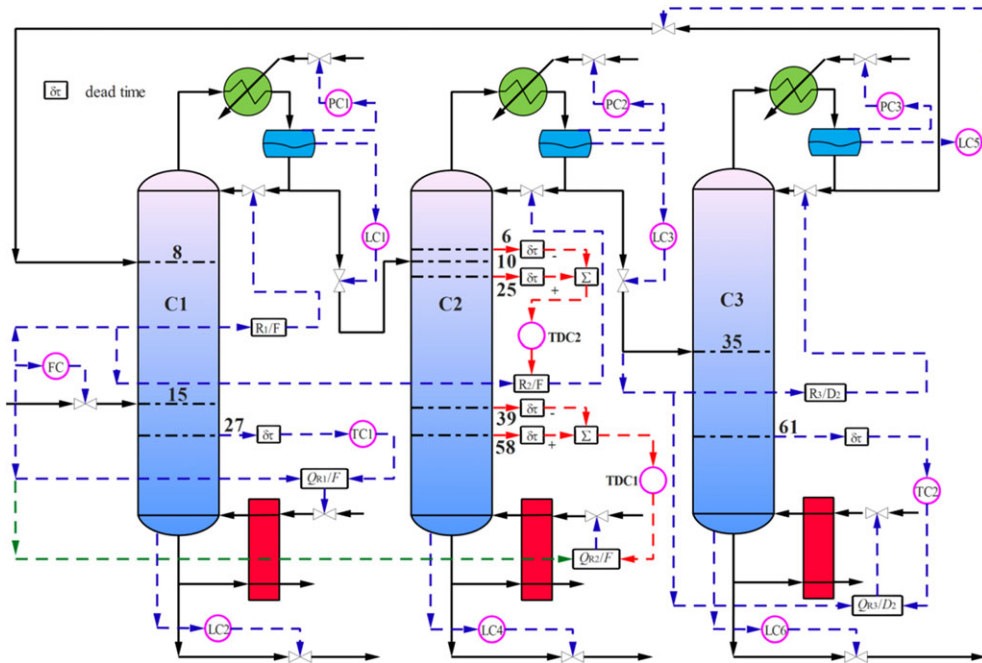


**Figure 9. Plant-wide control structure for triple-column pressure-swing distillation process.**  
 [Color figure can be viewed at [wileyonlinelibrary.com](http://wileyonlinelibrary.com)]

## Conclusions

In this work, we proposed a systematic procedure for optimal design and effective control of a triple-column pressure-swing distillation for separating ternary system with three binary minimum azeotropes. The thermodynamic feasibility insights were generated from the analysis of residue curve maps, which was successfully implemented into the process optimization using SA and SQP solvers. Optimal key operational parameters (e.g., feed location and reflux ratio) were thus generated with the lowest TAC of  $\$2.181 \times 10^6$  in sequence A. Next, a robust plant-wide control strategy with feedforward and dual temperature difference structure was proposed for the triple-column pressure-swing distillation process. It is demonstrated that product purities could be well maintained close to their set points using the proposed control structure when disturbances take places and hence the on-line composition measurement is not required.

The proposed systematic procedure involving process design, optimization, and control is well applicable to other multi-azeotrope systems with azeotrope(s) if concentration of azeotrope(s) changing significantly with pressures. Furthermore, the proposed robust plant-wide control strategy of triple-column pressure-swing distillation process is also applied to other separation process.

## Acknowledgment

The authors acknowledge the financial support provided by the National Natural Science Foundation of China (Nos. 21878028, 21606026); the Fundamental Research Funds for the Central Universities (No. 106112017CDJQJ228809); and Hundred Talents Program at Chongqing University. Helpful comments from the paper's reviewers and editor are also gratefully acknowledged.

## Literature Cited

1. He Z, Zhang B, Liang L, Lin S. Study on separating tetrahydrofuran from the mixture made up tetrahydrofuran, ethanol and water. *Shenyang Chem Ind.* 1995;4:30-32.
2. Zhao YT, Zhao TR, Jia H, Li X, Zhu ZY, Wang YL. Optimization of the composition of mixed entrainer for economic extractive distillation process in view of the separation of tetrahydrofuran/ethanol/water ternary azeotrope. *J Chem Technol Biotechnol.* 2017;92:2433-2444.
3. Luyben WL, Chien IL. *Design and control of distillation system for separating azeotropes.* London: Wiley Online Library; 2010.
4. Oliveiral SBM, Parise JAR, Pitanga Marques R. Modelling of an ethanol-water distillation column assisted by an external heat pump. *Int J Energy Res.* 2002;26(12):1055-1072.
5. Wang YL, Zhang Z, Zhang H, Zhang Q. Control of heat integrated pressure-swing distillation process for separating azeotropic mixture of tetrahydrofuran and methanol. *Ind Eng Chem Res.* 2015;54(5):1646-1655.
6. Luo BB, Feng HS, Sun DZ, Zhong X. Control of fully heat-integrated pressure swing distillation for separating isobutyl alcohol and isobutyl acetate. *Chem Eng Process.* 2016;110:9-20.
7. Luyben WL. Design and control of a fully heat-integrated pressure-swing azeotropic distillation system. *Ind Eng Chem Res.* 2008;47(8):2681-2695.
8. Lee J, Cho J, Dong MK, Sangjin P. Separation of tetrahydrofuran and water using pressure swing distillation: modeling and optimization. *Korean J Chem Eng.* 2011;28(2):591-596.
9. Wang YL, Zhang Z, Zhao YJ, Liang SS, Bu GL. Control of extractive distillation and partially heat-integrated pressure-swing distillation for separating azeotropic mixture of ethanol and tetrahydrofuran. *Ind Eng Chem Res.* 2015;54(34):8533-8545.
10. Wang YL, Bu G, Wang YK, Zhao TR, Zhang Z, Zhu ZY. Application of a simulated annealing algorithm to design and optimize a pressure-swing distillation process. *Comput Chem Eng.* 2016;95:97-107.
11. Zhu ZY, Xu DF, Jia H, Zhao YT, Wang YL. Heat integration and control of a triple-column pressure-swing Distillation process. *Ind Eng Chem Res.* 2017;56(8):2150-2167.
12. Wei HM, Wang F, Zhang JL, et al. Design and control of dimethyl carbonate-methanol separation via pressure-swing distillation. *Ind Eng Chem Res.* 2013;52(33):11463-11478.
13. Modla G, Lang P. Feasibility of new pressure-swing batch distillation methods. *Chem Eng Sci.* 2008;63(11):2856-2874.
14. Zhu ZY, Xu DF, Liu X, Zhang Z, Wang YL. Separation of acetonitrile/methanol/benzene ternary azeotrope via triple column pressure-swing distillation. *Sep Purif Technol.* 2016;169:66-77.
15. Luyben WL. Control of a triple-column pressure-swing distillation process. *Sep Purif Technol.* 2017;174:232-244.
16. Yang A, Lv LP, Shen WF, Dong LC, Li J, Xiao X. Optimal design and effective control of the *tert*-amyl methyl ether production process using an integrated reactive dividing wall and pressure swing columns. *Ind Eng Chem Res.* 2017;56(49):14565-14581.
17. Hsu KY, Hsiao YC, Chien IL. Design and control of dimethyl carbonate-methanol separation via extractive distillation in the dimethyl carbonate reactive-distillation process. *Ind Eng Chem Res.* 2010;49(2):735-749.
18. Qin JW, Ye Q, Xiong XJ, Li N. Control of benzene-cyclohexane separation system via extractive distillation using sulfolane as entrainer. *Ind Eng Chem Res.* 2013;52(31):10754-10766.
19. Shen WF, Dong LC, Wei SA, et al. Systematic design of an extractive distillation for maximum-boiling azeotropes with heavy entrainers. *AIChE J.* 2015;61(11):3898-3910.
20. Chen YC, Li KL, Chen CL, Chien IL. Design and control of a hybrid extraction distillation system for the separation of pyridine and water. *Ind Eng Chem Res.* 2015;54(31):7715-7727.
21. Rodríguez-Donis I, Gerbaud V, Joulia X. Thermodynamic insight on extractive distillation with entrainer forming new azeotropes. *Proc Distill Absorpt.* 2010;431-436.
22. Chien IL, Wang CJ, Wong DSH. Dynamics and control of a heterogeneous azeotropic distillation column: conventional control approach. *Ind Eng Chem Res.* 1999;38(2):468-478.
23. Luyben WL. Control of a multiunit heterogeneous azeotropic distillation process. *AIChE J.* 2006;52(2):623-637.
24. Luyben WL. Control of an azeotropic DWC with vapor recompression. *Chem Eng Process.* 2016;109:114-124.
25. Shen WF, Benyounes H, Gerbaud V. Extension of thermodynamic insights on batch extractive distillation to continuous operation. 1. azeotropic mixtures with a heavy entrainer. *Ind Eng Chem Res.* 2013;52(12):4623-4637.
26. Rodríguez-Donis I, Gerbaud V, Joulia X. Thermodynamic insights on the feasibility of homogeneous batch extractive distillation, 2. low-relative-volatility binary mixtures with a heavy entrainer. *Ind Chem Eng Res.* 2009;48(7):3560-3572.
27. Lang P, Kovacs G, Kotai B, Gaal-Szilagy J, Modla G. Industrial application of a new batch extractive distillation operational policy. *ICHEME Symp Ser.* 2006;152:830-839.
28. Lang P, Hegely L, Kovacs G, Gaal-Szilagy J, Kotai B. Solvent recovery from a multicomponent mixture by batch extractive distillation and hybrid process. *Proc Distill Absorpt.* 2010;295-300.
29. Seader JD, Henley EJ. *Separation Process Principles.* New York, NY: Wiley; 1998.
30. Doherty MF, Knapp JP. *Kirk-Othmer Encyclopedia of Chemical Technology.* John Wiley & Sons, Inc.; 2004.
31. Levy SG, Doherty MF. Design and synthesis of homogeneous azeotropic distillations. 4. Minimum reflux calculations for multiple-feed columns. *Ind Eng Chem Fund.* 1986;25(2):269-279.
32. Levy SG, Van Dongen DB, Doherty MF. Design and synthesis of homogeneous azeotropic distillation: 2. Minimum reflux calculations for nonideal and Azeotropic columns. *Ind Eng Chem Fund.* 1985;24(4):463-474.
33. Knapp JP, Doherty MF. Minimum entrainer flow for extractive distillation: a bifurcation theoretic approach. *AIChE J.* 1994;40(2):243-268.
34. Frits ER, Lelkes Z, Fonyo Z, Rev E, Markot MC. Finding limiting flows of batch extractive distillation with interval arithmetics. *AIChE J.* 2006;52(9):3100-3108.
35. Petlyuk F, Danilov R, Skouras S, Skogestad S. Identification and analysis of possible splits for azeotropic mixtures. 1. Method for column sections. *Chem Eng Sci.* 2011;66(12):2512-2522.
36. Petlyuk F, Danilov R, Skouras S, Skogestad S. Identification and analysis of possible splits for azeotropic mixtures. 2. Method for simple columns. *Chem Eng Sci.* 2012;69(1):159-169.

37. Modla G, Lang P. Separation of an acetone-methanol mixture by pressure-swing batch distillation in a double-column system with and without thermal integration. *Ind Eng Chem Res.* 2010;49(8):3785-3793.
38. Modla G, Lang P, Denes F. Feasibility of separation of ternary mixtures by pressure swing batch distillation. *Chem Eng Sci.* 2010;65(20):870-881.
39. Rodríguez-Donis I, Gerbaud V, Joulia X. Thermodynamic insights on the feasibility of homogeneous batch extractive distillation. 1. azeotropic mixtures with heavy entrainer. *Ind Chem Eng Res.* 2009;48(7):3544-3559.
40. Rodríguez-Donis I, Gerbaud V, Joulia X. Thermodynamic insights on the feasibility of homogeneous batch extractive distillation. 3. azeotropic mixtures with light boiling entrainer. *Ind Chem Eng Res.* 2012;51(2):4643-4660.
41. Rodríguez-Donis I, Gerbaud V, Joulia X. Thermodynamic insights on the feasibility of homogeneous batch extractive distillation. 4. azeotropic mixtures with intermediate boiling entrainer. *Ind Chem Eng Res.* 2012;51(18):6489-6501.
42. Kiva VN, Hilmen EK, Skogestad S. Azeotropic phase equilibrium diagrams: a survey. *Chem Eng Sci.* 2003;58(10):1903-1953.
43. Serafimov LA. The azeotropic rule and the classification of multicomponent mixtures VII. Diagrams for ternary mixtures. *Russ J Phys Chem.* 1970;44(4):567-571.
44. Knapp JP, Doherty MF. A new pressure-swing-distillation process for separating homogeneous azeotropic mixtures. *Ind Eng Chem Res.* 1992;31(1):346-357.
45. Douglas JM. *Conceptual Design of Chemical Processes.* New York, NY: McGraw-Hill; 1988.
46. Yang A, Wei RX, Sun SR, Shen WF, Chien IL. Energy-saving optimal design and effective control of heat integration-extractive dividing wall column for separating heterogeneous mixture methanol/toluene/water with multiazeotropes. *Ind Eng Chem Res.* 2018;57(23):8036-8056.
47. Ling H, Luyben WL. Temperature control of the BTX divided-Wall column. *Ind Eng Chem Res.* 2010;49(1):189-203.
48. Luyben WL. *Plantwide Dynamic Simulators in Chemical Processing and Control.* New York, NY: Marcel Dekker; 2002.
49. Luyben WL. *Distillation Design and Control Using Aspen Simulation.* 2nd ed. John Wiley; 2013.